Eur. Phys. J. B **50**, 475–481 (2006)
DOI: 10.1140/epjb/e2006-00158-1

THE EUROPEAN PHYSICAL JOURNAL B

Angular dependence of tunneling magnetoresistance in magnetic semiconductor heterostructures

A.A. Shokri[a]

[1] Department of Physics, Tehran Payame-Noor University, Fallahpour St. Nejatollahi St. Tehran, Iran
[2] Computational Physical Sciences Research Laboratory, Department of Nano-Science, Institute for studies in theoretical Physics and Mathematics (IPM) P.O. Box 19395-5531, Tehran, Iran

Received 29 October 2005
Published online 5 May 2006 – © EDP Sciences, Società Italiana di Fisica, Springer-Verlag 2006

Abstract. Theoretical studies on spin-dependent transport in magnetic tunnel heterostructures consisting of two diluted magnetic semiconductors (DMS) separated by a nonmagnetic semiconductor (NMS) barrier, are carried in the limit of coherent regime by including the effect of angular dependence of the magnetizations in DMS. Based on parabolic valence band effective mass approximation and spontaneous magnetization of DMS electrodes, we obtain an analytical expression of angular dependence of transmission for DMS/NMS/DMS junctions. We also examine the dependence of spin polarization and tunneling magnetoresistance (TMR) on barrier thickness, temperature, applied voltage and the relative angle between the magnetizations of two DMS layers in GaMnAs/GaAs/GaMnAs heterostructures. We discuss the theoretical interpretation of this variation. Our results show that TMR of more than 65% are obtained at zero temperature, when one GaAs monolayer is used as a tunnel barrier. It is also shown that the TMR decreases rapidly with increasing barrier width and applied voltage; however at high voltages and low thicknesses, the TMR first increases and then decreases. Our calculations explain the main features of the recent experimental observations and the application of the predicted results may prove useful in designing nano spin-valve devices.

PACS. 73.40.Gk Tunneling – 75.50.Pp Magnetic semiconductors – 73.23.Ad Ballistic transport

1 Introduction

In recent years, interest in tunneling of spin-polarized carriers through magnetic tunnel junctions (MTJs) has been partly fueled by the expectation that it can lead to novel microelectronics devices exploiting the spin degree of freedom of carriers as well as their charge. The MTJs are promising candidates for inclusion in magnetic random access memory, magnetic field sensors and quantum computing devices [1,2]. In most experiments, they consist of two ferromagnets separated by a nonmagnetic tunnel barrier. Junctions of this type including two magnetic layers, are named spin-valve devices. For such structures, tunneling magnetoresistance (TMR) arise due to different conductivity of parallel and antiparallel alignment of the magnetizations [3–5]. The magnitude of TMR depends on the spin polarizations of the two magnetic electrodes [6], but details remain to be worked out, particularly the role of spin-dependent scattering versus band structure.

Apart from the TMR observed in metallic MTJ, the spin-valve effect is also observed in semiconductor tunneling junctions. Because of a better compatibility with conventional microelectronics [7] and signature of the transmission of spin-polarized carriers [8], all-semiconductor spin-valves have an advantage. Using ferromagnetic semiconductors (FMSs), such as EuS, the TMR has also been investigated in single [9–12] and double [13–16] magnetic barrier junctions. In these structures, the FMSs, which act as spin filters, are used as tunnel barriers. Therefore, the MTJs based on these materials are able to produce highly spin-polarized current and high values of TMR. However, the Cure temperature in most of FMSs is much lower than the room temperature [17].

Moreover, recent progress has been made in manipulating the magnetic property that occurs in a number of common III-V compound semiconductors when some atoms are randomly replaced by magnetic atoms, such as Mn [18–20] of below critical temperature T_C. These materials are known as diluted magnetic semiconductors (DMSs). In DMSs, the exchange interaction between the itinerant carriers in the semiconducting band and the localized spins on magnetic impurity ions leads to spectacular magneto-optical effects, such as giant Faraday rotation or Zeeman splitting. To achieve large spin polarization

[a] e-mail: aashokri@nano.ipm.ac.ir

in DMSs, the Zeeman splitting of the conduction (valence) band must be high for electrons (holes), this depends upon the concentration of magnetic species. For a type of III–V compound, the discovery of a higher T_C about 110 K in GaAs based ferromagnetic semiconductor, $Ga_{1-c}Mn_cAs$, with optimal Mn concentration $c \sim 0.05$ [18] has generated much attention. GaMnAs is a good candidate for DMS properties due to the relatively high T_C, the spontaneous magnetization and the feasibility of preparing GaAs-based DMSs. The origin of ferromagnetism in the GaMnAs can be demonstrated through the *p-d* exchange coupling between the itinerant holes in the valence band of GaAs and the spin of Mn magnetic impurities [18,20,21]. Hence, in recent years, the spin-dependent transport phenomena in the MTJs based on $Ga_{1-c}Mn_cAs$/(GaAs or AlAs) heterostructures have been studied by several groups [22–24]. Also, Tao et al. [25] studied the AlAs thickness dependence of TMR using the transfer matrix approach. Their treatment, is however somewhat questionable, because they did not apply the boundary conditions for derivatives of wave functions correctly. When the materials are different, it is the normal mass flux that must be continuous.

In this paper, we develop the analytical studies on coherent spin-polarized transport in GaMnAs/GaAs/GaMnAs heterostructures by considering the effects of angular dependence of the magnetization of electrodes of the DMS layers along the lines of our recent work [26]. It may be suitable to identify the origin of TMR for a superlattice structure with such layers. Here, we emphasis the variation of magnetization between two DMS electrodes which can be rotated by a small applied field. This effect may be considered because in some experiments, spin conservation no longer holds, and the spin-flip scattering may affect the transport properties [27]. Next, we propose a formula to obtain the spin-dependent transmission through the structure. Using the Landauer-Büttiker formalism [28] we will calculate the tunneling current density and then study the TMR and spin polarization of tunneling carriers in terms of the barrier thickness and applied voltage at all temperatures.

The rest of the paper is organized as follows. To understand the spin-polarized tunneling results for DMS/NMS/DMS heterostructures, we invoke the model based on quantum theory and then the spin polarization and the TMR are formulated in Section 2. In our model, spins of electrons during tunneling are no supposed be conserved, namely, the tunneling of spin-up and spin-down electrons are not an independent process. In Section 3, numerical results obtained for a new typical tunnel junction (GaMnAs/GaAs/GaMnAs) are discussed, while the paper is summarized in Section 4.

2 Theoretical framework

In this section, we investigate the spin-dependent transport properties in a new type of MTJ based on DMS materials by including the angular dependence of magnetizations in the DMSs. The structure consists of two semi-infinite DMS electrodes separated by a NMS layer, in the presence of applied voltage V_a. For simplicity, we assume that the two DMS electrodes are made of the same material and all the interfaces are flat shown in Figure 1. Based on the parabolic valence band effective mass approximation and spontaneous magnetization of DMS electrodes [26], we obtain an analytical expression for the angular dependence of transmission in DMS/NMS/DMS junctions. The longitudinal part of the one-hole Hamiltonian can be written as

$$H_x = -\frac{\hbar^2}{2m_j^*}\frac{d^2}{dx^2} + U_j(x) - \mathbf{h}_j^{\mathrm{MF}} \cdot \sigma, \tag{1}$$

where m_j^* (j = 1–3) is the hole effective mass in the jth layer, and

$$U_j(x) = \begin{cases} 0, & x < 0 \\ E_{\mathrm{F}} + \phi - eV_{\mathrm{a}}x/t_{\mathrm{bar}}, & 0 < x < t_{\mathrm{bar}} \\ -eV_{\mathrm{a}}, & x > t_{\mathrm{bar}}, \end{cases} \tag{2}$$

where t_{bar} is the barrier thickness, E_{F} is the Fermi energy in the left electrode, measured from the middle point between the edges of the two spin subbands, and ϕ is the barrier height measured from the Fermi level. $-\mathbf{h}_j^{\mathrm{MF}} \cdot \sigma$ is the internal exchange energy where $\mathbf{h}_j^{\mathrm{MF}}$ is the molecular field in the jth DMS electrode and σ is the conventional Pauli spin operator.

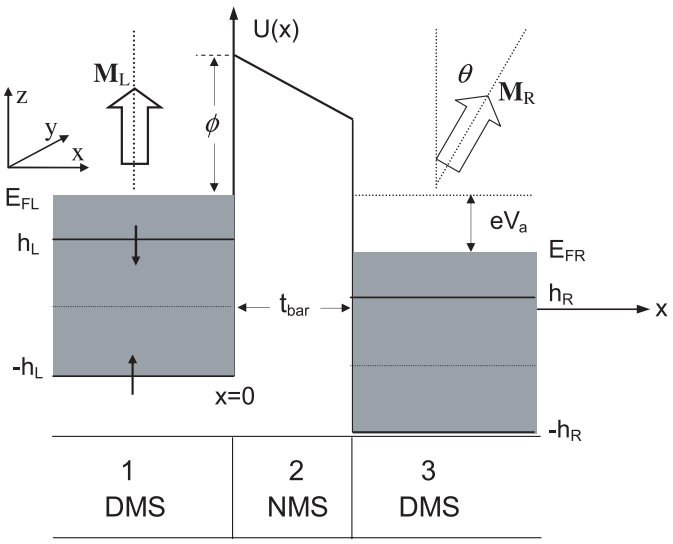

Fig. 1. Spin-dependent potential profile for DMS/NMS/DMS magnetic heterostructures under forward bias V_a. t_{bar} is the barrier thickness, $E_{\mathrm{FL(FR)}}$ is the Fermi energy in the left (right) electrode, measured from the middle point between the edges of two spin subbands, and ϕ is the barrier height measured from the Fermi level. The angle θ is the relative angle between the magnetization of two DMS electrodes. The zero of energy is taken at the middle of bottoms for majority-spin band and minority-spin one in the left DMS electrode. The presented MTJ profile is at $T < T_{\mathrm{C}}$, which the spin-splitting energy is non zero.

The Schrödinger equation for a biased barrier layer can be simplified by a coordinate transformation whose solution is the linear combination of the Airy function Ai[$\rho(x)$] and its complement Bi[$\rho(x)$] [29]. Considering all three regions of the DMS/NMS/DMS junction, the eigenfunctions of the Hamiltonian (1) with eigenvalue E_x have the following forms:

$$\psi_j(x) = \begin{cases} A_{1\uparrow}e^{ik_{1\uparrow}x} + B_{1\uparrow}e^{-ik_{1\uparrow}x} + A_{1\downarrow}e^{ik_{1\downarrow}x} \\ \qquad +B_{1\downarrow}e^{-ik_{1\downarrow}x}, x < 0 \\ A_{2\uparrow}\mathrm{Ai}[\rho(x)] + B_{2\uparrow}\mathrm{Bi}[\rho(x)] + A_{2\downarrow}\mathrm{Ai}[\rho(x)] \\ \qquad +B_{2\downarrow}\mathrm{Bi}[\rho(x)], 0 < x < t_{\mathrm{bar}} \\ A_{3\uparrow}e^{ik_{3\uparrow}x} + B_{3\uparrow}e^{-ik_{3\uparrow}x} + A_{3\downarrow}e^{ik_{3\downarrow}x} \\ \qquad +B_{3\downarrow}e^{-ik_{3\downarrow}x}, x > t_{\mathrm{bar}}, \end{cases} \quad (3)$$

where

$$k_{1\sigma} = \sqrt{2m_1^*(E_x + h_0\sigma)}/\hbar \quad (4)$$

$$k_{3\sigma} = \sqrt{2m_3^*(E_x + eV_{\mathrm{a}} + h_0\sigma)}/\hbar, \quad (5)$$

are the hole wave vectors along the x axis. Here, σ are the hole spin components ± 1 (or $\uparrow, \downarrow$), and $h_0 = |\mathbf{h}_j^{\mathrm{MF}}|$, $(j = 1, 3)$. The temperature dependence of the molecular field h_0 in the DMS electrodes is calculated before [26], using mean-field theory. The coefficients $A_{j\sigma}$ and $B_{j\sigma}$ are constants to be determined from the boundary conditions, while

$$\rho(x) = -\frac{d}{eV_{\mathrm{a}}\lambda}\left(E_{\mathrm{F}} + \phi - E_x - \frac{x}{t_{\mathrm{bar}}}eV_a\right), \quad (6)$$

with

$$\lambda = \left[\frac{-\hbar^2 t_{\mathrm{bar}}}{2m_2^* eV_{\mathrm{a}}}\right]^{1/3}. \quad (7)$$

Our system has translation asymmetry in the direction perpendicular to the growing direction x. Therefore, the transverse momentum $\mathbf{k}_\parallel$ is omitted from the above notations, namely, the summation over $\mathbf{k}_\parallel$ is carried out in our calculations.

Upon applying the boundary conditions such that the wave functions and their first derivatives are matched at $x = 0$ and t_{bar}, we obtain a matrix of the coefficients of ψ_1 and ψ_3. These boundary conditions at $x = 0$ are $\psi_1(0) = \psi_2(0)$ and $(m_1^*)^{-1}[d\psi_1(0)/dx] = (m_2^*)^{-1}[d\psi_2(0)/dx]$, and also, the change in quantization axis at $x = t_{\mathrm{bar}}$ requires the spinor transformation

$$\begin{aligned} \psi_{2\uparrow}(t_{\mathrm{bar}}) &= \psi_{3\uparrow}(t_{\mathrm{bar}})\cos(\tfrac{\theta}{2}) + \psi_{3\downarrow}(t_{\mathrm{bar}})\sin(\tfrac{\theta}{2}), \\ \psi_{2\downarrow}(t_{\mathrm{bar}}) &= -\psi_{3\uparrow}(t_{\mathrm{bar}})\sin(\tfrac{\theta}{2}) + \psi_{3\downarrow}(t_{\mathrm{bar}})\cos(\tfrac{\theta}{2}) \end{aligned} \quad (8)$$

and, similarly for the derivatives.

The matrix formula can be written as

$$\begin{bmatrix} A_{1\uparrow} \\ B_{1\uparrow} \\ A_{1\downarrow} \\ B_{1\downarrow} \end{bmatrix} = \mathbf{M} \begin{bmatrix} A_{3\uparrow} \\ B_{3\uparrow} \\ A_{3\downarrow} \\ B_{3\downarrow} \end{bmatrix}, \quad (9)$$

where, $\mathbf{M}$ is the total transfer matrix.

For holes with spin-up incident from the left electrode, we have $A_{1\uparrow} = 1$, $A_{1\downarrow} = 0$, and $B_{3\uparrow} = B_{3\downarrow} = 0$, (since there is no reflection in region 3) so, the transmitted amplitudes are obtained from equation (9) as

$$A_{3\uparrow} = \frac{M_{33}}{M_{11}M_{33} - M_{13}M_{31}}, \; A_{3\downarrow} = -\frac{M_{31}}{M_{11}M_{33} - M_{13}M_{31}}. \quad (10)$$

Therefore, if a spin-up hole tunnels from left DMS electrode into right electrode and occupies the spin-up and spin-down states of the right electrode, the corresponding transmission coefficients, are defined as the ratio of the transmitted flux to the incident flux, are given by

$$T_{\uparrow\uparrow}(\theta) = |A_{3\uparrow}|^2|\tfrac{m_1^* k_{3\uparrow}}{m_3^* k_{1\uparrow}}|, \; T_{\uparrow\downarrow}(\theta) = |A_{3\downarrow}|^2|\tfrac{m_1^* k_{3\downarrow}}{m_3^* k_{1\uparrow}}| \quad (11)$$

respectively. Similarly, for holes with spin-down incident from the left electrode, we have $A_{1\uparrow} = 0$, $A_{1\downarrow} = 1$, $B_{3\uparrow} = B_{3\downarrow} = 0$, and thus,

$$A_{3\uparrow} = -\frac{M_{13}}{M_{11}M_{33} - M_{13}M_{31}}, \; A_{3\downarrow} = \frac{M_{11}}{M_{11}M_{33} - M_{13}M_{31}}. \quad (12)$$

Here, the transmission coefficients of spin-down incident electrons as spin-up $T_{\downarrow\uparrow}(\theta)$, and spin-down $T_{\downarrow\downarrow}(\theta)$, are as

$$T_{\downarrow\uparrow}(\theta) = |A_{3\uparrow}|^2|\tfrac{m_1^* k_{3\uparrow}}{m_3^* k_{1\downarrow}}|, \; T_{\downarrow\downarrow}(\theta) = |A_{3\downarrow}|^2|\tfrac{m_1^* k_{3\downarrow}}{m_3^* k_{1\downarrow}}|. \quad (13)$$

On the other hand, from equation (9), the elements of total transfer matrix, M_{11}, M_{33}, M_{13} and M_{31}, can be derived, analytically

$$\begin{aligned} \mathrm{M}_{11} &= S_1\cos(\tfrac{\theta}{2}), \;\; \mathrm{M}_{33} = S_3\cos(\tfrac{\theta}{2}), \\ \mathrm{M}_{13} &= S_2\sin(\tfrac{\theta}{2}), \; \mathrm{M}_{31} = -S_4\sin(\tfrac{\theta}{2}), \end{aligned} \quad (14)$$

where

$$S_1 = \frac{\pi}{2}\left[(\beta + \frac{m_1^*}{ik_{1\uparrow}}\delta) - \frac{ik_{3\uparrow}}{m_3^*}(\alpha + \frac{m_1^*}{ik_{1\uparrow}}\gamma)\right]e^{ik_{3\uparrow}t_{\mathrm{bar}}}, \quad (15)$$

$$S_2 = \frac{\pi}{2}\left[(\beta + \frac{m_1^*}{ik_{1\uparrow}}\delta) - \frac{ik_{3\downarrow}}{m_3^*}(\alpha + \frac{m_1^*}{ik_{1\uparrow}}\gamma)\right]e^{ik_{3\downarrow}t_{\mathrm{bar}}}, \quad (16)$$

$$S_3 = \frac{\pi}{2}\left[(\beta + \frac{m_1^*}{ik_{1\downarrow}}\delta) - \frac{ik_{3\downarrow}}{m_3^*}(\alpha + \frac{m_1^*}{ik_{1\downarrow}}\gamma)\right]e^{ik_{3\downarrow}t_{\mathrm{bar}}}, \quad (17)$$

$$S_4 = \frac{\pi}{2}\left[(\beta + \frac{m_1^*}{ik_{1\downarrow}}\delta) - \frac{ik_{3\uparrow}}{m_3^*}(\alpha + \frac{m_1^*}{ik_{1\downarrow}}\gamma)\right]e^{ik_{3\uparrow}t_{\mathrm{bar}}}. \quad (18)$$

Here, the following abbreviations are used

$$\alpha = (\lambda m_2^*)\{\mathrm{Ai}[\rho(0)]\mathrm{Bi}[\rho(t_{\mathrm{bar}})] - \mathrm{Bi}[\rho(0)]\mathrm{Ai}[\rho(t_{\mathrm{bar}})]\}, \quad (19)$$

$$\beta = \mathrm{Ai}[\rho(0)]\mathrm{Bi}'[\rho(t_{\mathrm{bar}})] - \mathrm{Bi}[\rho(0)]\mathrm{Ai}'[\rho(t_{\mathrm{bar}})], \quad (20)$$

$$\gamma = \mathrm{Ai}'[\rho(0)]\mathrm{Bi}[\rho(t_{\mathrm{bar}})] - \mathrm{Bi}'[\rho(0)]\mathrm{Ai}[\rho(t_{\mathrm{bar}})], \quad (21)$$

$$\delta = \frac{1}{\lambda m_2^*}\{\mathrm{Ai}'[\rho(0)]\mathrm{Bi}'[\rho(t_{\mathrm{bar}})] - \mathrm{Bi}'[\rho(0)]\mathrm{Ai}'[\rho(t_{\mathrm{bar}})]\}, \quad (22)$$

where, $\mathrm{Ai}'[\rho(x)]$ and $\mathrm{Bi}'[\rho(x)]$ are the first derivatives of the Airy functions.

With above considerations, the tunneling spin-dependent current densities, $J_{\sigma\sigma'}$, with $\sigma(\sigma') = \uparrow$ and $\downarrow$ for a MTJ with a given applied bias $V_{\rm a}$ at temperature T can be calculated within the nearly-free-hole approximation [28]:

$$J_{\sigma\sigma'}(\theta, V_{\rm a}) = \frac{em_1^* k_B T}{4\pi^2\hbar^3} \int_{E_0}^{\infty} T_{\sigma\sigma'}(E_x, \theta, V_{\rm a}) \times \ln\left\{\frac{1+\exp\left[(E_{\rm F}-E_x)/k_BT\right]}{1+\exp\left[(E_{\rm F}-E_x-eV_{\rm a})/k_BT\right]}\right\} dE_x \ , \quad (23)$$

and, at $T = 0$ K,

$$J_{\sigma\sigma'}(\theta, V_{\rm a}) = \frac{em_1^*}{4\pi^2\hbar^3}\left[eV_{\rm a}\int_{E_0}^{E_{\rm F}-eV_{\rm a}} T_{\sigma\sigma'}(E_x, \theta, V_{\rm a})dE_x + \int_{E_{\rm F}-eV_{\rm a}}^{E_{\rm F}} (E_{\rm F}-E_x)T_{\sigma\sigma'}(E_x, \theta, V_{\rm a})dE_x\right], \quad (24)$$

where k_B is the Boltzmann constant and E_0 is the lowest possible energy that allows transmission and is given by $E_0 = h_0$, for spin-up and -down holes. It is clear that, the tunnel currents are modulated by the magnetic configurations of the both DMS electrodes.

The degree of spin polarization in each configuration is defined as

$$\mathrm{P}(\theta) = \frac{J_\uparrow(\theta) - J_\downarrow(\theta)}{J_\uparrow(\theta) + J_\downarrow(\theta)} \ , \quad (25)$$

where, $J_{\uparrow(\downarrow)} = \sum_\sigma J_{\uparrow\sigma(\downarrow\sigma)}$, and σ are the spin electron $\uparrow$ and $\downarrow$. For studying the TMR, a measurable quantity, we calculate the tunnel conductance per unit area, $G(\theta, V_a) = \sum_{\sigma\sigma'} J_{\sigma\sigma'}(\theta, V_{\rm a})/V_{\rm a}$. Therefore, the angular dependence of the TMR can be described quantitatively by the relative change of the conductance with respect to the different orientation of magnetic moment in DMS electrodes as

$$\mathrm{TMR}(\theta) = \frac{G(0) - G(\theta)}{G(\theta)} \ , \quad (26)$$

where, $G(0)$ corresponds to the conductances in the parallel alignments of the magnetizations in the DMS layers. In the following, the numerical results on the effects spin-dependent transport on the spin polarization and the TMR in a typical DMS/NMS/DMS tunnel heterostructures are presented.

3 Numerical results and discussions

Numerical calculations are performed for a typical $Ga_{1-c}Mn_cAs/GaAs/Ga_{1-c}Mn_cAs$ tunnel heterostructures. We have chosen $Ga_{1-c}Mn_cAs$ and GaAs because they have the same crystal structure and the lattice mismatch is very small [23]. The lattice constant a_0, and Fermi energy $E_{\rm F}$ are taken as 5.65 Å, and 200 meV [23] for $Ga_{1-c}Mn_cAs$ electrodes, respectively. Other relevant parameters are the same as those used in Ref. [26] for a sample with $T_{\rm C} = 110$ and $c = 0.05$. The calculations presented in this paper were done for the barrier height of GaAs, $\phi = 100$ meV, which can be found in the relevant literature [30]. The effective mass of all carriers for the structure are taken is $m^* = 0.16m_e$ [26], where m_e is the free-hole mass.

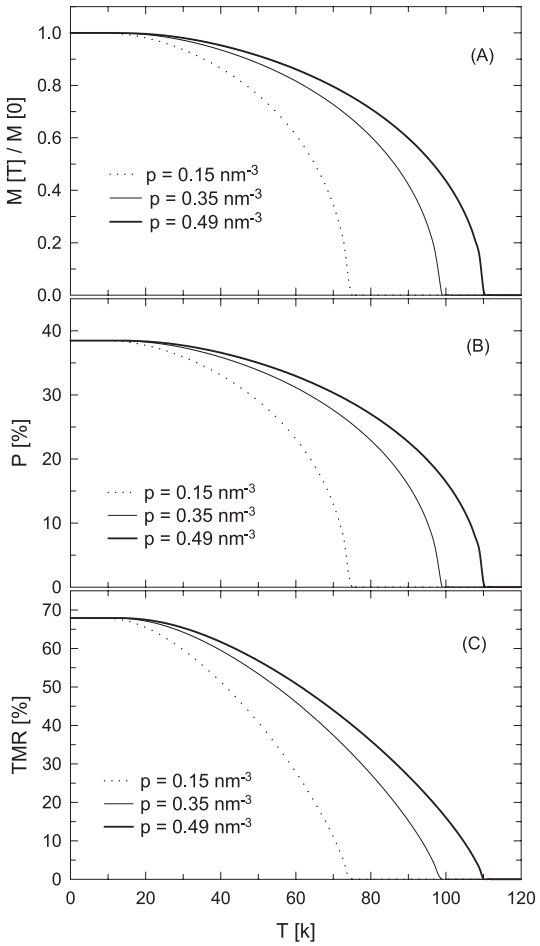

Fig. 2. Dependence of (A) the normalized magnetization of $Ga_{0.95}Mn_{0.05}As$ electrodes, (B) the itinerant-hole spin polarization, and (C) the TMR in the GaMnAs/GaAs/GaMnAs tunnel junctions as a function of temperature for several different hole densities, $p = 0.15$, 0.35, and 0.49 nm^{-3} with the fixed values of $V_{\rm a} = 5$ mV, and $t_{\rm bar} = 0.565$ nm.

According to Figure 1, in our MTJ, the magnetization direction of the left DMS electrode stays fixed, but the spin orientation of the right DMS electrode is free and may be switched from 0 to 2π with respect to the left DMS magnetization direction by an external magnetic field. In the following, we give the numerical results on the effects of barrier thickness, temperature, applied voltage and relative angle between the magnetizations of the two DMS electrodes on the spin polarization and the TMR.

In Figures 2 and 3, we have shown the temperature dependence of the normalized Mn-ion magnetization of $Ga_{1-c}Mn_cAs$, the itinerant-hole spin polarization and the TMR for the GaMnAs/GaAs/GaMnAs tunnel junctions at several values of the hole densities p and Mn-ion concentrations c, respectively. In Figure 2, the curves have been plotted when $p = 0.15$, 0.35, and 0.49 nm^{-3} with the

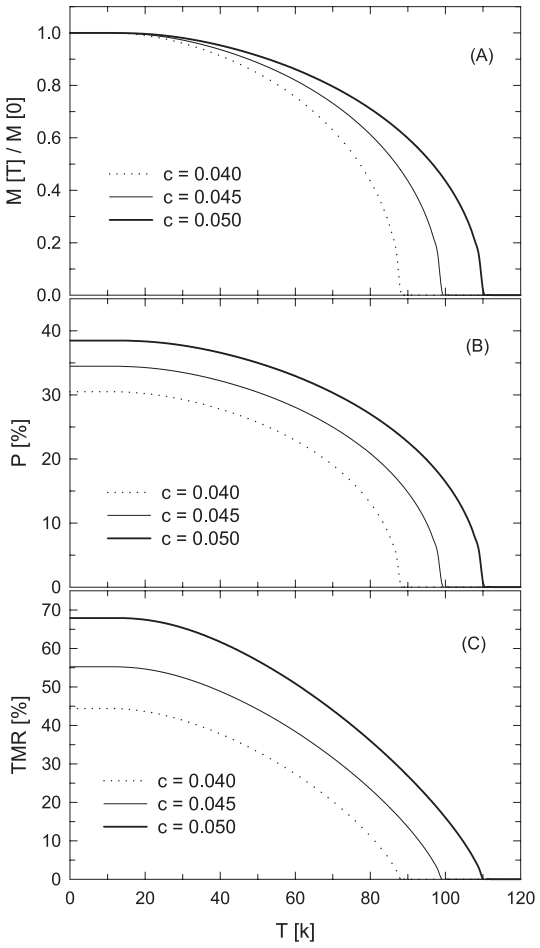

Fig. 3. Dependence of (A) the normalized magnetization of $Ga_{1-c}Mn_cAs$ electrodes, (B) the itinerant-hole spin polarization, and (C) the TMR in the GaMnAs/GaAs/GaMnAs tunnel junctions as a function of temperature for several different Mn-ion concentrations, $c = 0.040$, 0.045, and 0.05 with the fixed value of $p = 0.49$ nm^{-3}. Other parameters are taken the same as those in Figure 2.

fixed values of $c = 0.05$, $V_a = 5$ mV, and $t_{bar} = 0.565$ nm. It is obvious that the critical temperature T_C increases when the hole density increases because T_C exhibits a non-monotonic dependence on p (see Eq. (25) in Ref. [26]), therefore, the values of T_C corresponding to $p = 0.15, 0.35$, and 0.49 nm^{-3}, are found to 74, 98, and 110 K, respectively. It is clear from Figure 2A that the magnetization of the DMS electrode vanishes in above the critical temperature, which is due to disappearance of the valence band spin-splitting energy at $T \geq T_C$. The highest value of spin polarization can reach 38% at zero temperature for different hole densities, which makes the TMR about 70%. With increasing temperature, these values reduce to zero, when $T \geq T_C$. Also, it is observed that the magnetization, the spin polarization and the TMR decrease rapidly for lower hole densities when the temperature increases. The origin of this effect is related to the reduction of band splitting Δ between the spin-up and -down states in valence band of $Ga_{1-c}Mn_cAs$, when hole densities decrease at $T \leq T_C$.

Table 1. The extracted values of the critical temperature T_C, the highest spin polarization P, and the TMR (at zero temperature) from Figure 3, for several Mn-ion concentration c with the fixed values of $p = 0.49$ nm^{-3}, $V_a = 5$ mV, and $t_{bar} = 0.565$ nm.

c	0.040	0.045	0.050
T_C	88	99	110
P(%)	31	34	37
TMR(%)	44	55	68

It is necessary to point out that, the ferromagnetic coupling strength between the Mn-ion spins in $Ga_{1-c}Mn_cAs$ becomes weaker when the hole density decreases [21], and so, the spin polarization and the TMR are both reduced.

The features in Figure 3 are plotted for several different Mn-ion concentrations, $c = 0.040$, 0.045, and 0.050, with the fixed values of p =0.49 nm^{-3}, $V_a = 5$ mV, and t_{bar} =0.565 nm. It is clear that the critical temperature T_C reduces when impurity Mn-ion concentration decreases (see Eq. (25) in Ref. [26] and also Tab. 1). However, similar to what we have discussed before, the temperature dependence of the magnetization (Fig. 3A) is related to the value of the spin-splitting of the DMS electrodes. Contrary to Figure 2, one can see that the highest value of spin polarization and also TMR at zero temperature do not become equal for different c's (see Tab. 1). With increasing temperature, the spin polarization and TMR reduce to zero, when $T \geq T_C$. Also, it is seen that the magnetization, the spin polarization and the TMR decrease rapidly for lower impurity Mn-ion concentrations, when temperature increases. The origin of this effect is also related to the strength of ferromagnetic coupling between the Mn-ion spins in $Ga_{1-c}Mn_cAs$, which in low Mn-ion concentrations is weak, and so, the spin polarization is induced, partially. But the strength of the ferromagnetic coupling become strong when the doping of Mn increases in $Ga_{1-c}Mn_cAs$ and the itinerant holes becomes spin-polarized, completely. This result creates a larger spin polarization and TMR at higher temperatures below T_C (see Figs. 3A and 3B).

We also calculated the dependence of TMR on the relative angle between the magnetization of two electrodes with different applied voltages at $T = 0$ K, and $t_{bar} = 0.565$ nm, and plotted the tunneling current densities at $V_a = 5$ mV and at $V_a = 80$ mV, in Figures 4A and 4B, respectively. Figure 4C displays the dependence of the TMR on angle θ. When the magnetic moments of two DMS electrodes are parallel ($\theta = 0$), the tunneling current density for $J_{\uparrow\downarrow}$ is zero, the same for $J_{\downarrow\uparrow}$, and therefore there is no spin-flip effect. On the other hand, in the antiparallel alignment ($\theta = \pi$), $J_{\uparrow\uparrow}$ and $J_{\downarrow\downarrow}$ are zero, and the spin flip effect is very important. For other angles, all components of tunneling current densities change and become nonzero. Continuing to increase the angle from $\theta = \pi$ to 2π, the variation of the tunneling current densities show similar behavior as that from $\theta = 0$ to π. The origin of this effect can be understood by the effect of angular dependence of the magnetizations in DMSs, which

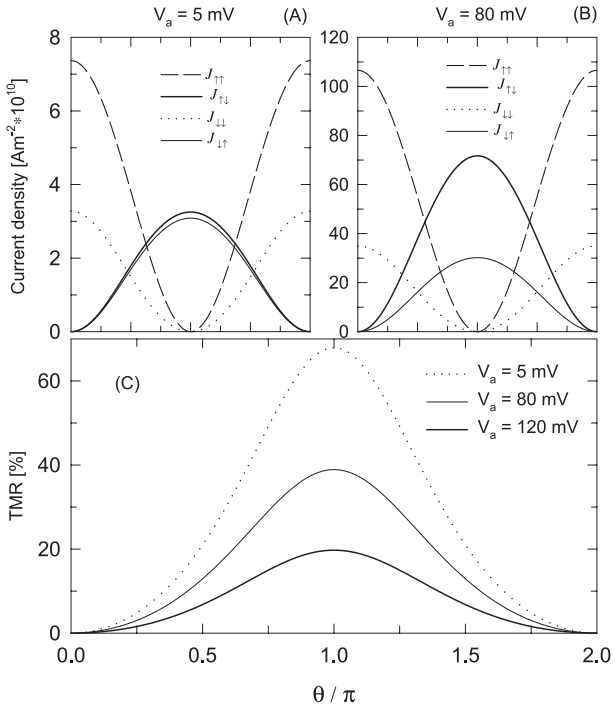

Fig. 4. Variation of the tunneling current densities and TMR on the relative angle between the magnetization of two electrodes at different barrier thickness for several applied voltage at $T = 0$ K with the fixed values of $c = 0.05$, $p = 0.49$ nm^{-3}, and $t_{\rm bar} = 0.565$ nm.

changes the sign of transmitted hole spin through the system. It is observed that values of tunneling current densities with $V_{\rm a} = 80$ mV in Figure 4B are bigger than the corresponding currents in Figure 4A. The reason for this is related to the tilt of the barrier potential under an applied voltage. At low voltages, the tunneling current densities vary linearly, but with increasing the applied voltage, the effective width of the barrier becomes narrower and a nearly parabolic dependence of current on the voltage appears [12,31]. As the applied voltage increases the difference between the normalized current densities in parallel state ($\theta = 0$), and an arbitrary (θ) configuration decreases, and then, the TMR is reduced (see Fig. 4C), namely, the spin filter effect becomes weak. Figure 4C also shows that the highest value of TMR (about 70%) is obtained in $V_{\rm a} = 5$ mV, when the relative angle becomes $\theta = \pi$ (antiparallel alignment) at zero temperature. This value reduces to nearly 20% in $V_{\rm a} = 120$ mV. Also, it is found that the the TMR increases, monotonically, when the angle increases, while Figure 4 shows the TMR exhibits the spin-valve effect.

In the pervious work [26], we investigated the dependence of TMR on the barrier thickness for different applied voltage in GaMnAs/GaMn/GaMnAs heterostructures without applying the effect of angular dependence of the magnetizations in DMS. We also obtained that with enhancement of the applied voltage by more than the barrier height (100 meV) a quantum well will appear at GaAs/GaMnAs interface. Therefore, the carriers can

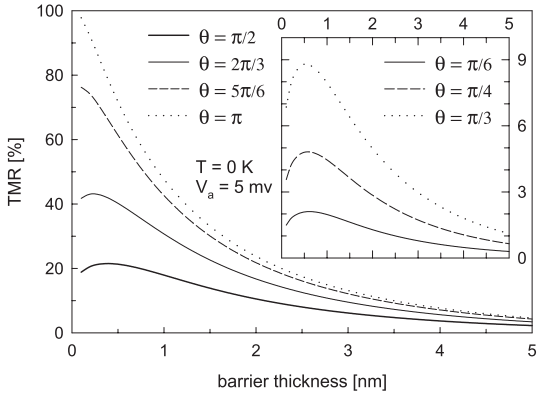

Fig. 5. Dependence of the TMR on the relative angle between the magnetization of two electrodes at different barrier thickness at $T = 0$ K with the fixed values of $c = 0.05$, $p = 0.49$ nm^{-3}, and $V_{\rm a} = 5$ mV.

cause standing waves in the barrier, leading to not only a change of the magnitude of the TMR, but also its sign switching from positive to negative when the thickness increases. The reduction of TMR is due to tilt of the barrier potential, under an applied voltage, when the spin filter effect becomes weak. In this regard, we have displayed the TMR as a function of the barrier thickness $t_{\rm bar}$ for seven different angles between two magnetic moments of the DMS, at zero temperature and $V_{\rm a} = 5$ mV in Figure 5, which shows an interesting behavior. It is seen that, the TMR first rises and then decreases when $t_{\rm bar}$ increases, that is, the TMR exhibits a peak in the thinner barrier region, which has been observed experimentally by Tanaka and Higo [23]. The location of this maximum shifts toward low thickness when the angle θ increases and then disappears. When $t_{\rm bar}$ increases, the peaks are gradually invisible. Also, with increasing the applied voltage, the peaks of TMR has shifted toward low thickness when θ deviates from 0 to π. The physical explanation of this behavior is related to the resonance transmission coefficients $T_{\uparrow\uparrow}$, $T_{\uparrow\downarrow}$, $T_{\downarrow\downarrow}$, and $T_{\downarrow\uparrow}$, when the difference between the spin polarization in the parallel magnetization configuration and the angle θ between two magnetization of electrodes first increases and then decreases when $t_{\rm bar}$ increases. It is necessary to point out that with increasing the barrier thickness, the transmission, spin polarization and tunneling currents decrease (e.g. see [1]).

Therefore, the calculated results show that, the temperature dependent spin transport is a result of the ferromagnetic phase of the DMS electrodes, and by adjusting the temperature, applied voltage and the barrier thickness, one can reach high values for the tunneling spin-polarization and TMR. It is expected that the enhanced TMR effects and its interesting behavior will have potential applications.

4 Conclusions

On the basis of the parabolic valence band effective mass approximation, we have obtained an analytical expression for the angular dependence of transmission for

DMS/NMS/DMS tunnel junctions by including the angular dependence of magnetizations in DMSs. The dependence of spin polarization of itinerant holes and the TMR on the applied voltage, barrier width and the angle between two magnetizations of $Ga_{1-c}Mn_cAs$ at all temperatures and for several Mn concentrations were investigated in the $Ga_{1-c}Mn_cAs/GaAs/Ga_{1-c}Mn_cAs$ heterostructures. We have shown that the TMR first increases and then decreases when the barrier thickness increases, which exhibits a peak at low thickness. This peak is clear at small angles. They decrease with increasing temperature and can be controlled by doping of Mn in GaMnAs. Our calculations explain the main features of the recent experimental observations and also show the possibility of new semiconductor device with an added functionality of magnetic multilayers, so it may be useful in designing spin-valve devices in the future [20].

The author is grateful to Dr A. Saffarzadeh for helpful discussions and also Prof. H. Rafii-Tabar for critical reading of the manuscript.

References

1. J.S. Moodera, L.R. Kinder, T.M. Wong, R. Meservey, Phys. Rev. Lett. **74**, 3273 (1995)
2. J. Daughton, J. Appl. Phys. **81**, 3758 (1997)
3. J.C. Slonczewski, Phys. Rev. B **39**, 6995 (1989)
4. E.Y. Tsymbal, D.G. Pettifor, J. Phys.: Condens. Matter **9**, L411 (1997)
5. K. Wang, S. Zhang, P.M. Levy, L. Szunyogh, P. Weinberger, J. Magn. Magn. Mater. **189**, L131 (1998)
6. M. Jullière, Phys. Lett. A **54**, 225 (1975)
7. D.D. Awschalom, D. Loss, N. Samarth, in *Semiconductor Spintronics and Quantum Computation* (Springer- Verlag, Berlin-Heidelberg, 2002)
8. E.Y. Tsymbal, O.N. Mryasov, P.R. LeClair, J. Phys.: Condens. Matter **15**, R109 (2003)
9. P. LeClair, J.K. Ha, H.J.M. Swagten, J.T. Kohlhepp, C.H. van de Vin, W.J.M. de Jonge, Appl. Phys. Lett. **80**, 625 (2002)
10. A. Saffarzadeh, J. Magn. Magn. Mater. **269**, 327 (2004)
11. A.A. Shokri, A. Saffarzadeh, J. Phys.: Condens. Matter **16**, 4455 (2004)
12. A.A. Shokri, A. Saffarzadeh, Eur. Phys. J. B **42**, 187 (2004)
13. D.C. Worledge, T.H. Geballe, J. Appl. Phys. **88**, 5277 (2000)
14. A.T. Filip, P. LeClair, C.J.P. Smits, J.T. Kohlhepp, H.J.M. Swagten, B. Koopmans, W.J.M. de Jonge **81**, 1815 (2002)
15. A. Saffarzadeh, J. Phys.: Condensed Matter **15**, 3041 (2003)
16. M. Wilczyński, J. Barnaś, R. Świrkowicz, J. Magn. Magn. Mater. **267**, 391 (2003)
17. A. Mauger, C. Godart, Phys. Rep. **141**, 51 (1986)
18. H. Ohno, Science **281**, 951 (1998); H. Ohno, J. Magn. Magn. Matter. **200**, 110 (1999)
19. H. Ohno, D. Chiba, F. Matsukura, T. Omiya, E. Abe, T. Dietl, Y. Ohno, K. Ohtani, Nature (London) **408**, 944 (2000)
20. T. Dietl, H. Ohno, F. Matsukura, J. Cibert, D. Ferrand, Science **287**, 1019 (2000); B. Lee, T. Jungwirth, A.H. MacDonald, Semicond. Sci. Technol. **17**, 393 (2002)
21. J. König J, H.-H. Lin, A.H. MacDonald, Phys. Rev. Lett. **84**, 5628 (2000)
22. D. Chiba, N. Akiba, F. Matsukura, Y. Ohno, H. Ohno, Appl. Phys. Lett. **77**, 1873 (2000)
23. M. Tanaka, Y. Higo, Phys. Rev. Lett. **87**, 026602 (2001)
24. T. Hayashi, M. Tanaka, A. Asamitsu, J. Appl. Phys. **87**, 4673 (2000)
25. Y.C. Tao, J.G. Hu, H. Liu, J. Appl. Phys. **96**, 498 (2004)
26. A. Saffarzadeh, A.A. Shokri, J. Magn. Magn. Matter. (2006), in press
27. R. Meservey, P.M. Tedrow, Phys. Rep. **238**, 173 (1994); M.A.M. Gijs, G.E.W. Bauer, Adv. Phys. **46**, 285 (1997); J.M. De Teresa, A. Barthelemy, A. Fert, J.P. Contour, R. Lyonnet, F. Montaigne, P. Seneor, A. Vaurès, Science **286**, 507 (1999), and references therein
28. C.B. Duke, in *Tunneling Phenomena in Solids*, edited by E. Burstein, S. Lundquist (New York, Plenum, 1969)
29. M. Abramowitz, I.A. Stegun, in *Handbook of Mathematical Functions* (New York, Dover, 1965)
30. D. Chiba, F. Matsukara, H. Ohno, Physica E **21**, 966 (2004)
31. W.F. Brinkman, R.C. Dynes, J.M. Rowell, J. Appl. Phys. **41**, 1915 (1970)